Shielding properties investigation of impact-initiated energetic materials under hypervelocity impact

Qiang Wu(1), Qingming Zhang(2), Zizheng Gong(1) ,Kunbo Xu(1) ,Renrong Long(2)

(1) *Beijing Institute of Spacecraft Environment Engineering, Beijing 100094, China, Email:wuqiang12525@126.com*
(2) *State Key Laboratory of Explosion Science and Technology, Beijing Institute of Technology, Beijing 100081, China*

ABSTRACT

In this paper, a series of experiments have been performed on a new whipple shield structure which consists of an Al/PTFE(polytetrafluoroethylene) bumper by using two-stage light gas gun at velocities between 3.71 and 6.08 km/s. Good protection of shield is obtained through comparative experiments which used the same bumper areal density. The results show that the critical projectile diameter can be increased by 20.5%-45%. In order to reveal the protective mechanism of new concept shield, the perforation characteristics of PTFE/Al bumper and shadowgraph of debris are analyzed. The results suggest that shock initiation characteristics of energetic material under impact enhanced the debris shield performance.

Key words: hypervelocity impact; Al/PTFE energetic material; perforation characteristics; protection mechanism

1   Introduction

Due to the increasing population of orbital debris in near Earth environments, the required performance of meteoroid and orbital debris (M/OD) protection systems for future manned vehicles can be expected to increase. In order to meet protection requirements of various types spacecraft, many enhanced shield configurations have been designed based on whipple shield, extensive experimental and computational investigations also have been carried out[1-8]. Although many materials are applied to shield structures, they are all inert materials. Since the fragmentation mechanism of the inert materials is single, protective capability for large size debris is restricted.

This paper presents a space debris shield structure with Al/PTFE energetic material. Al/PTFE is a kind of impact-initiated energetic materials which integrate desirable characteristics of high energy density and rapid energy release properties[9]. Currently, all research are concentrating on how to enhance the damage effect of warhead by using the impact initiation characteristics of Al/PTFE[10-12]. However, study on hypervelocity impact characteristics of Al/PTFE energetic material has not been reported.

2   Hypervelocity impact experiment

2.1   Fabrication of PTFE/Al bumper

The metal/PTFE energetic composite is a kind of advanced energetic material. In this research, the average initial particle sizes were 25um and 3um for the PTFE and Al, respectively. The stoichiometric mixture of 76.5wt% PTFE and 23.5wt% Al was chosen. Then the mixture powders were prepared by cold press and sintering method. As bumper of a shield, the strength of Al/PTFE was hoped the higher the better. The previous research has indicated that the appropriate molding pressure is 80MPa, and combined with sintering process curve which has melting and crystal platform, as shown in Fig. 1, the Al/PTFE can get an optimal mechanical property.
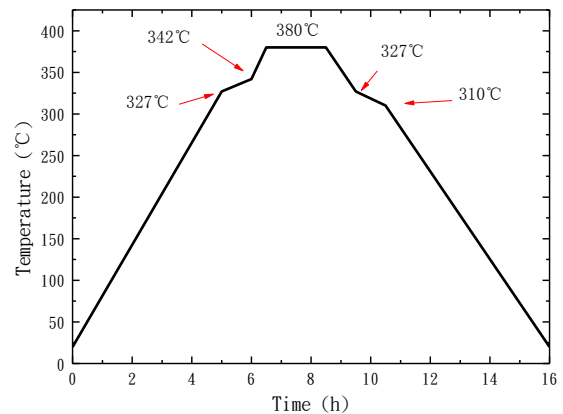

Figure 1. Sintering process curve with melting and crystal platform

To ensure the comparative experiments have the same bumper areal density, material parameters need to satisfy the following relations:

$$\rho_{Al} h_{Al} = \rho_0 h_0 \qquad （1）$$

Where ρ_{Al} and h_{Al} are the density and thickness of aluminum bumper, ρ_0 and h_0 are the density and thickness of Al/PTFE bumper.

After pressing, the pressed Al/PTFE shape undergoes a sintering cycle. Accompanying with voids crushing and internal stress release, sintering allows the particles to fuse together to form a homogeneous material. For the volume of materials will be changed before and after sintering, it's difficult to determine the ρ_0 or h_0 separately. Eq. 2 gives a formula for calculating the

mass required for the preparation of energetic materials, where R is the dies radius:

$$M = \pi R^2 \rho_0 h_0 \qquad (2)$$

Bring the Eq. 1 into 2, the M can be written as,

$$M = \pi R^2 \rho_{Al} h_{Al} \qquad (3)$$

Therefore, in order to ensure the same areal density, we only need to determine the required material quality. The areal density error of the Al/PTFE sheet is less than 1% by this method. Examples of Al/PTFE sheet are given in Fig. 2.

Figure 2. Examples of Al/PTFE sheet: diameter=110mm

2.2 Experimental method and results

All of the experiments were performed using a two-stage light gas gun with the bumper normal to the range center line and combining with experimental measures of high speed photography, optical pyrometer and laser shadow photography. The projectiles were LY-12 Al spheres with a diameter ranging from 5.0 mm to 6.4mm.

A schematic of the energetic whipple shield during the test is given in Fig. 3. In order to ensure the integrity of the spherical projectile, a pneumatic separation system was used to separate the projectile and sabot, in which way a satisfactory separation effect was achieved. Fig. 4 shows a typical sabot used in the experiment and the contrast of interception target before and after impact by

the sabot. Hypervelocity impact tests have been completed at BIT State Key Laboratory of Explosion Science and Technology(SKLEST). Tab. 1 provides experimental configurations and results for hypervelocity impact tests on energetic materials shield concept.

Figure 3. Whipple shield configuration: layout and composition, standoff=10cm
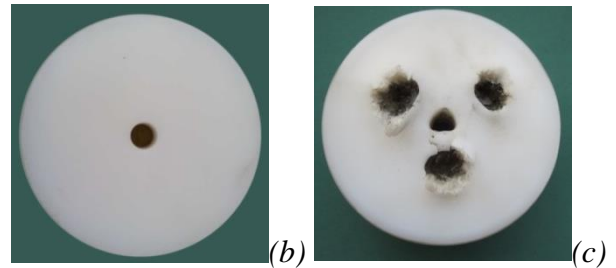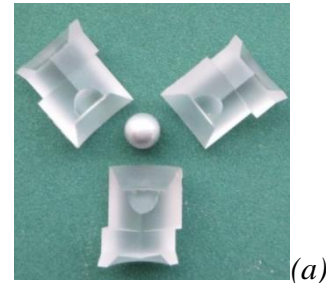

Figure 4. A typical sabot (a) and contrast of interception target before (b) and after (c) impact

Table1 Hypervelocity impact test configurations and rear wall damage results

Test No.	Projectile parameters			Whipple shield configuration				Rear Wall damage results
	d_p (mm)	m_p (g)	v_p (km/s)	Bumper Material	Bumper AD (g/cm^2)	Rear Wall material	t_w (mm)	
1	6.4	0.38	5.13	Al2024	1.11	Al2024	4	P
2	6.4	0.38	5.09	Al/PTFE	1.11	Al2024	4	NP, slight bulge
3	6.4	0.38	5.06	Al2024	0.84	Al2024	4	P

4	6.4	0.38	5.03	Al/PTFE	0.84	Al2024	4	NP, slight DS
5	5	0.18	3.88	Al/PTFE	0.84	Al2024	4	NP, bulge
6	5	0.18	3.79	Al/PTFE	0.84	Al2024	4	NP, bulge
7	5	0.18	4.0	Al/PTFE	0.84	Al2024	4	NP, slight bulge
8	6	0.31	3.71	Al/PTFE	0.84	Al2024	4	P
9	6.4	0.38	6.08	Al/PTFE	0.84	Al2024	4	NP, slight bulge

Note: AD stands for areal density, t_w represents the thickness of rear wall, P stands for perforation and NP means no perforation, DS stands for detached spall.

3 Discussion

3.1 Comparative experiments

The Experiment 1 and 2 were performed as a group of comparative experiments in which bumper's areal density are 1.11 g/cm2. The characteristic damages of the rear wall are shown in Fig. 5. For the experiment 1, on the front face there are two large holes and deep pits are all around the holes, the number of deep pits whose diameter are bigger than 3mm is about 57. On the back face, holes and spalling are both evident. The number of bumps is about 19. For the front face of Experiment 2, the number of deep pits whose diameter are bigger than 3mm reduced sharply to 15, and there is no penetration or any spalling on the back face. Bump number is only 5, and the shield structure is still in a valid state.
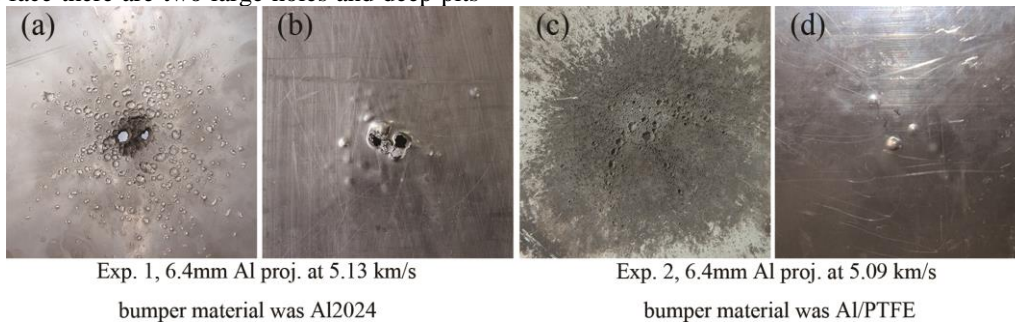

Exp. 1, 6.4mm Al proj. at 5.13 km/s
bumper material was Al2024

Exp. 2, 6.4mm Al proj. at 5.09 km/s
bumper material was Al/PTFE

Figure 5. Comparison of damage on rear wall for the configurations with AD=1.11 g/cm2: front face (a) and back face (b) correspond to the experiment 1; front face (c) and back face (d) correspond to the experiment 2

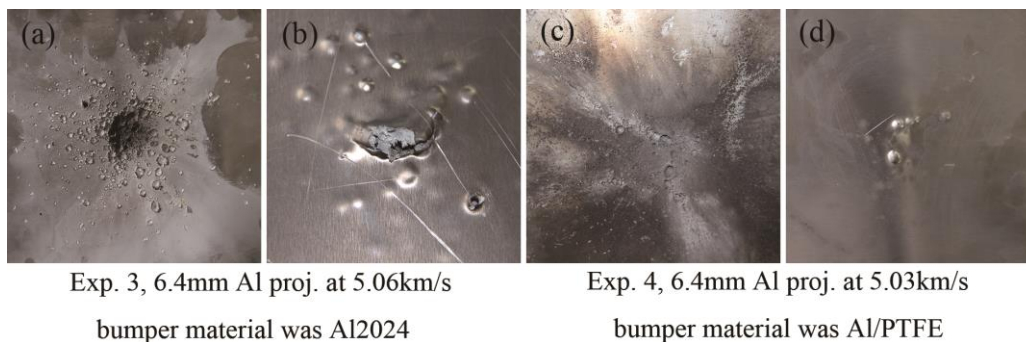Exp. 3, 6.4mm Al proj. at 5.06km/s
bumper material was Al2024

Exp. 4, 6.4mm Al proj. at 5.03km/s
bumper material was Al/PTFE

Figure 6. Comparison of damage on rear wall for the configurations with AD=0.84 g/cm2: front face (a) and back face (b) correspond to the experiment 3; front face (c) and back face (d) correspond to the experiment 4

Fig. 6 shows comparison of damage on rear wall for the configurations with AD=0.84 g/cm^2. For the experiment 3, there is a serious damage zone around 25mm in diameter on the front face, and the number of deep pits

whose diameter are bigger than 3mm is about 46. On the back face, spalling is obvious and there is a tear area around 10mm in length. The number of bumps is about 17. In the comparative experiment 4, there are only 13 deep pittings on the front face with no penetration. The spalling is very slight on back face, and the shield structure is in a critical state. Fig. 7 shows the number of deep pits on front face for comparative experiments 1-4.
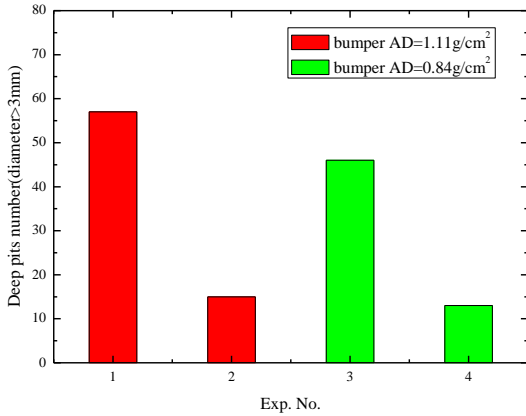

Figure 7. The number of deep pits on front face for comparative experiments 1-4.

3.2 Perforation characteristics of PTFE/Al bumper

Fig. 8 shows a typical perforation characteristics of the Al/PTFE bumper in test 2. It is evident that the Al/PTFE energetic material does not have self-sustained reaction characteristics like a traditional explosive. This feature is beneficial to the protection applications on spacecraft.

Figure 8. Perforation in the Al/PTFE bumper: Test No.2, Vp=5.09 km/s

Different from the inert material perforation forming process, Al/PTFE energetic material will occur shock initiation reaction under impact, which changed the expanding mechanism. Therefore, the diameter of perforation is not only related to the kinetic energy of the projectile, but also related to the shock initiation characteristics of the Al/PTFE. Figure 8 indicate that perforation stopped when it reaches a few times the diameter of the projectile. Because Al/PTFE energetic materials do not have self-sustaining reaction characteristics, it can be inferred that the perforation process can be divided into three stages under

hypervelocity impact (as shown in Fig. 9): shock detonation stage, fracture and deflagration stage, spalling and fracture stage.
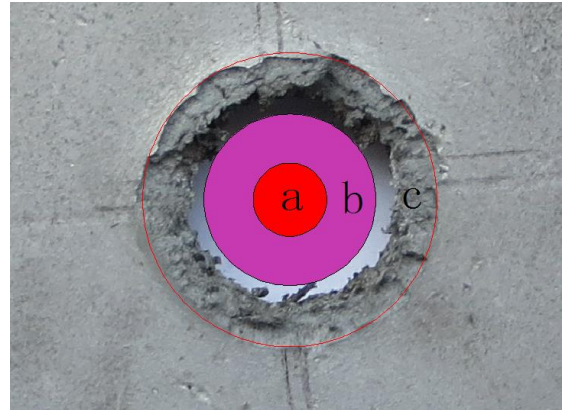

Figure 9. Schematic diagram of Al/PTFE bumper perforation: (a) Shock detonation area, (b) Fracture and deflagration area, (c) Spalling and fracture area

(1)Shock detonation area: A transient high pressure was generated by the impact of projectile, part kinetic energy of projectile transfer into inner energy rapidly. After reaching the threshold for reaction, the chemical energy release instantly like detonation. Corresponding perforation zone is a shock detonation area, as shown in Figure 9 (a). It has been proved that the Al/PTFE 1 can undergo a detonation reaction under the pressure of more than 15Gpa [13].

(2)Fracture and deflagration area: The shock wave propagation along the radial direction in Al/PTFE bumper is close to a spherical wave. Due to the weakening effect of surface rarefaction wave, the Al/PTFE will fracture first instead of detonation immediately. When the delayed ignition time was achieved, the chemical energy release in the form of deflagration. Corresponding perforation zone is a Fracture and deflagration area, as shown in Figure 9 (b). The Al/PTFE energy release rate decreased significantly with the reaction ratio is less than 1.

(3)Spalling and fracture area: The shock wave intensity decreases with the increase of the radial distance. Although the Al/PTFE can still be broken, the internal energy deposit in the material is not enough to cause any chemical reaction. This part of the material will be broken in the form of debris. Corresponding perforation zone is a spalling and fracture area, as shown in Figure 9 (c).

The pyrometer signal and high speed camera results in the experiment proved the correctness of the above analysis. Fig. 10 shows a typical pyrometer measurement result in test 2 and the pyrometer optical probe placed between the Al/PTFE bumper and the rear wall. As can be seen from the graph, the temperature changes in a double-peak structure, while the maximum

temperature of the first peak is 3825K and the second peak temperature is only 2870K. The maximum value of first peak corresponding to the detonation reaction of the shock detonation area while falling edge corresponding to the deflagration reaction of fracture and deflagration area，where energy release rate decreased gradually. The second peak was generated by unreacted fragments of Al/PTFE impact the rear wall which correspond to spalling and fracture area. Fig. 11 is the corresponding image field after impact where lots of tiny pieces of debris floating around. For it has been long enough after impact, the debris are all come from the Al/PTFE bumper but not projectile which correspond to spalling and fracture area.
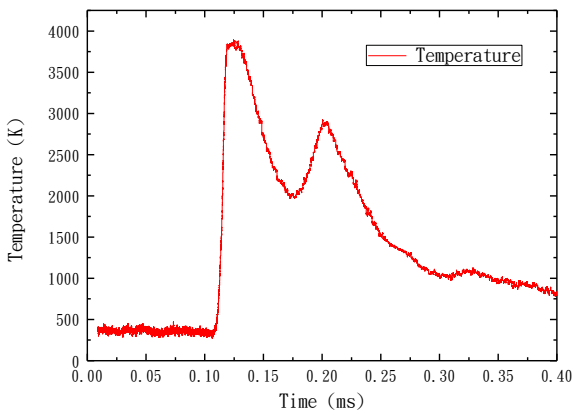

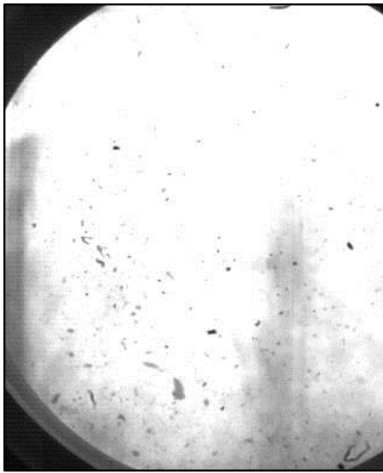*Figure 10. The typical pyrometer measurement result in test 2*

Figure 11. The typical high speed images in test 2

3.3　Ballistic limit analysis

Ballistic limit curves are functions of material strength, shield spacing, projectile size, shape and density, as well as a number of other variables. The "Christiansen" equations are the most widely used double-plate predictor equation published by JSC[14], and includes the results from additional aluminum alloy projectile and target hypervelocity impact test.

Experiment 4 indicates that a 6.4mm aluminum projectile impacting at 5.03 km/s cause the shield to it's critical state. Since the critical projectile diameter for the Al2024 bumper is 5.04mm through the "Christiansen" equations, protective ability of Al/PTFE energetic material bumper is enhanced by about 28%. For the experiment 5~7, projectile diameter was reduced to 5mm, and impact velocity were 3.79~4.0km/s, shields were all in a valid state. When the projectile diameter increased to 6mm at 3.71 km/s in the experiment 8, shields was in a failure state. The only difference between experiment 4 and 9 was the impact velocity: experiment 9 at 6.08 km/s has a better ballistic performance than the experiment 4 at 5.03 km/s.

Fig. 12 illustrates the ballistic limit curves(BLC) which was fitted by using the least square method. By contrast with the conventional Al2024 shield, the Al/PTFE energetic material bumper can make a sharp increase in protective capability for the shield.
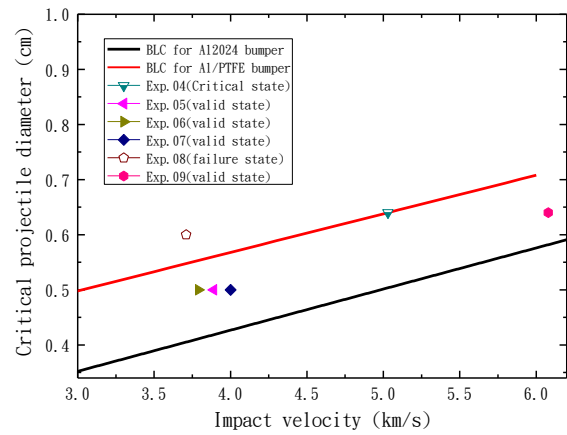

Figure 12. Comparison of improved BLC in this study vs. Christiansen BLC for Whipple Shield with aluminum Projectile at 0-degree Impact Angle.

3.4　Protection mechanism analysis

The function of the bumper is to break up the projectile into a cloud of material containing both projectile and bumper. This cloud expands while moving across the standoff, resulting in the impactor momentum being distributed over a wide area of the rear wall. At the same time, the impact can also cause some of the debris to melt and vaporization, thereby further reducing the damage effect on the rear wall. Therefore, we can study the protective mechanism of the protective structure by analyzing the morphological characteristics of debris cloud.

The debris shadowgraphs of test 3 and 4 are shown in Fig. 13. In shadowgraph of test 3, solid particles can be seen clearly, but not in test 4. This is because the initiation reaction of Al/PTFE occurs instantaneously under the hypervelocity impact, and the projectile debris are surround by the gaseous product.
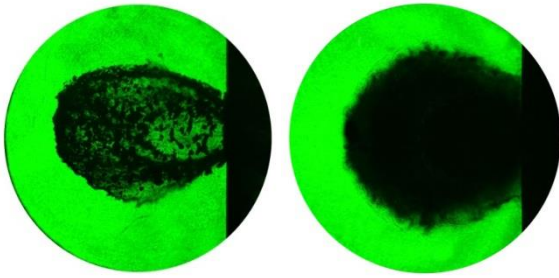
Figure 13. The debris shadowgraphs of test 3 and 4

The phase transition effect of the conventional inert material shield depends on the residual specific energy and the impact velocity is closely related. However, the phase transition effect of energetic materials is related to their own chemical energy. The shock induced reaction product of Al/PTFE is gaseous, which can significantly reduce the number of solid debris in the debris cloud. The results show that the phase transition effect of the material during the hypervelocity impact process can effectively reduce the damage ability of the debris cloud to the rear wall[15].

Due to the strong energy release characteristics of the energetic material under impact, the total pressure produced by the impact not only includes the pressure caused by shock compression, but also the pressure caused by the instantaneous release of chemical energy. The two kinds of impact pressure together to enhance the projectile crush degree. According to the theory of the shock wave heating, the increase of the total impact pressure is beneficial to increase the residual specific energy of the projectile and promote the melting and vaporization of the projectile. Generally, solids in the debris cloud are more penetrating in the rear wall than the liquid or gaseous phase materials[16].

Moreover, since there is almost no air medium in the space, the explosion reaction would not produce a shock wave to destroy the rear wall.

4   Conclusion

The potential application of Al/PTFE energetic material bumper is discussed for a whipple-type shield in this paper. Hypervelocity impact experiments are conducted to compare the protection efficiency of conventional aluminium bumper by normal impact of spherical aluminium projectile with velocity of 3-6km/s. Al/PTFE energetic material bumper prove to be display better protection efficient than traditional aluminium bumper when shock initiation reaction is induced. The Al/PTFE energetic material bumper can break-up the projectile into smaller, less massive, slower projectiles due to the combined effect of impact and explosion, thereby significantly enhanced the spacecraft protection ability. The purpose of the research is to provide a concept using explosion reaction in order to improve protection against micrometeoroid and orbital debris impacts on future space-based systems.

References

1. Cour-Palais, B.G. & Crew, J.L. (1990). A Multi-Shock Concept for Spacecraft Shielding. International Journal of Impact Engineering. 10, 135-146.

2. Zhang, Q.M. & Long, R.R. (2008). A model for debris clouds produced by impact of hypervelocity projectiles on multiplate structures .Applied Physics Letters. 108(10),101903.

3. Christiansen, E.L. & Kerr, J.H. (1993). Mesh Double-bumper Shield: A Low-weight Alternative for Spacecraft Meteoroid and Orbital Debris Protection. International Journal of Impact Engineering. 14, 169-180.

4. Maclay, T.D., Culp, R.D. & Bareiss, L. (1993). Topographically Modified Bumper Concepts for Spacecraft Shielding. International Journal of Impact Engineering. 14, 479-489.

5. Christiansen, E.L., Crews, J.L. & Williamsen, J.E. (1995). Enhanced Meteoroid and Orbital Debris Shielding. International Journal of Impact Engineering. 17, 217-228.

6. Christiansen, E.L. & Kerr, J.H. (1999). Flexible and Deployable Meteoroid/Debris Shielding for Spacecraft. International Journal of Impact Engineering. 3(11), 125-136.

7. Giffin, A., Shneider, M.N. & Miles, R.B. (2010). Potential micrometeoroid and orbital debris protection system using a gradient magnetic field and magnetic flux compression. Applied Physics Letters. 94, 054102.

8. Hou, M.Q., Gong, Z.Z. & Xu, K.B. (2014). Experimental study on hypervelocity impact characteristics of density-grade thin-plate. Acta Phys. Sin. 63,024701.

9. Zhang, X.F., Shi, A.S. & Qiao, L. (2013). Experimental study on impact-initiated characters of multifunction energetic structural materials. Journal of Applied Physics. 113,083508.

10. Nielson, D.B. & Tanner, R.L. (2007). High Strength Reactive Materials and Methods of Making. US: 7307117B2.

11. Wang, H.F., Zheng, Y.F. & Yu, Q.B. (2011). Impact-induced initiation and energy release behavior of reactive materials. Journal of applied Physics. 110,074904.

12. Ames, R. (2006). Proceedings of Materials Research Society Symposium, Boston, pp. 78-83.

13. Guo, J., Zhang, Q.M. & Zhang, L.S. Reaction behavior of polytetrafluoroethylene/AL granular composites subjected to planar shock wave. Propellants, Explosives, Pyrotechnics, 201600115.

14. Christiansen, E.L. (11993). Design and Performance Equations for Advanced Meteoroid and Debris Shield. International Journal of Impact Engineering. 14, 145-156.

15. Hopkins, A.K., Lee, T.W. & Swift, H.F. (1972). Material Phase Transformation Effects upon Performance of Spaced Bumper Systems. Journal of Spacecraft and Rockets. 9(5), 342-345.

16. Christiansen, E.L. (2006). Meteoroid/Debris Shielding (U.S. Government Printing Office, Houston) p.43.